Author(s): Lipiäinen, Lauri & Jaakkola, Antti & Kokkonen, Kimmo & Kaivola, Matti

Title: Frequency splitting of the main mode in a microelectromechanical resonator due to coupling with an anchor resonance

Year: 2012

Version: Final published version

Please cite the original version:

Lipiäinen, Lauri & Jaakkola, Antti & Kokkonen, Kimmo & Kaivola, Matti. 2012. Frequency splitting of the main mode in a microelectromechanical resonator due to coupling with an anchor resonance. Applied Physics Letters. Volume 100, Issue 1. 013503. ISSN 1077-3118 (electronic). ISSN 0003-6951 (printed). DOI: 10.1063/1.3673558.

Frequency splitting of the main mode in a microelectromechanical resonator due to coupling with an anchor resonance

Lauri Lipiäinen, Antti Jaakkola, Kimmo Kokkonen, and Matti Kaivola

Citation: Applied Physics Letters **100**, 013503 (2012); doi: 10.1063/1.3673558
View online: http://dx.doi.org/10.1063/1.3673558
View Table of Contents: http://scitation.aip.org/content/aip/journal/apl/100/1?ver=pdfcov
Published by the AIP Publishing

Frequency splitting of the main mode in a microelectromechanical resonator due to coupling with an anchor resonance

Lauri Lipiäinen,[1,a] Antti Jaakkola,[2] Kimmo Kokkonen,[1] and Matti Kaivola[1]
[1]*Department of Applied Physics, Aalto University, P.O. Box 13500, FI-00076 AALTO Espoo, Finland*
[2]*VTT Technical Research Centre of Finland, P.O. Box 1208, FI-02044 VTT Espoo, Finland*

(Received 23 August 2011; accepted 9 December 2011; published online 4 January 2012)

We present an experimental study of the frequency scaling of the main, square-extensional mode in a piezoelectrically actuated plate resonator. The studied set consists of resonators of different plate sizes with identical anchors. The behavior of the square-extensional mode is analyzed using electrical impedance measurements and optical characterization of the mechanical vibration fields. The results reveal a detrimental anchor effect, where for certain plate sizes the square-extensional mode branch is split into two due to a coupled oscillation of the resonator plate and the anchors. © *2012 American Institute of Physics*. [doi:10.1063/1.3673558]

Recent progress in microelectromechanical systems (MEMS) technology has opened up possibilities for the use of single-crystal silicon resonators in frequency control and timing applications, dominated for decades by quartz crystal based components. The foreseen benefits of MEMS resonators include, e.g., low cost, compact size, low power consumption, and added functionality due to compatibility with complementary metal-oxide-semiconductor (CMOS) processing. It has already been demonstrated that capacitively driven square-extensional (SE) mode MEMS resonators can fulfill the performance requirements for frequency reference applications.[1] There is a further interest to excite MEMS resonators piezoelectrically[2,3] in order to avoid the need for bias voltage and sub-100-nm sized gaps as in capacitive excitation.

In a MEMS resonator, the energy has to be mechanically well confined within the resonating structure. Since anchoring is needed to support the resonator, the whole device structure, including the anchors, should be carefully designed to minimize the leakage of acoustic energy to the surroundings. Both analytical[4] and numerical[5] methods exist to calculate such structures, but in practice, empirical testing is often required to truly optimize a device. Experimental studies of the anchoring geometry of bulk mode MEMS resonators[6–8] suggest that in order to minimize the acoustic loss, the anchors should be flexible and preferably be located at the nodal points of the vibration mode.

In SE-mode operation, the resonator plate expands and contracts, while preserving its shape and, therefore, does not have a nodal point at the plate perimeter. As the in-plane (IP) vibration component of the SE mode contains most of the vibration energy, the existing nodal point of the IP vibration at the center of the plate would be an optimal anchor site. Unfortunately, anchoring at this point is challenging in the type of resonators discussed here,[3] in which the SE mode is excited using a piezoelectric thin film on top of the resonator plate, see Fig. 1(a). In our resonators, the anchors are therefore placed at the plate corners. Even though in this design the SE mode vibration maxima fall at the anchor positions, it has been demonstrated that a high quality-factor SE resonance ($Q \approx 130\ 000$) can be achieved in a capacitively excited SE mode resonator, using such an anchor structure.[1]

In this letter, we present an experimental study of the frequency scaling of the SE vibration mode as a function of the resonator plate size. A starting point for the analysis was the measurements of the electrical response of a set of 1200 MEMS resonators.[9] It was observed that, at certain device sizes, the SE mode branch appeared to split into two distinct frequency branches. In order to gain physical insight into

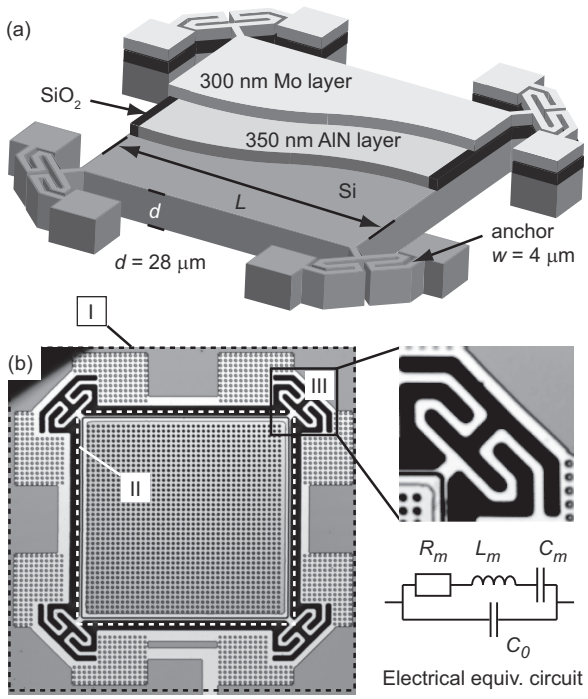

FIG. 1. (a) Structure of the square-plate resonator. The 28-μm-thick, single-crystalline silicon resonator plate is attached to the substrate at the plate corners with 4-μm-wide meander anchors. A 350-nm-thick piezoelectric AlN layer is deposited on top of the plate. A 300-nm Mo layer on top of the AlN layer acts as a top electrode, and the Si resonator plate itself acts as a bottom electrode. (b) Photograph of the $L = 209\ \mu$m resonator sample and the rectangular scan areas I (scan step 1.54 μm), II (0.44 μm), and III (0.44 μm) used for laser probe measurements. To enable in-plane laser probe measurements, the top-electrode Mo layer is patterned with a 5-μm grid of circular 2.5-μm-diameter holes. The electrical equivalent circuit model of the resonator is shown at the bottom-right corner.

[a]Electronic mail: lauri.lipiainen@tkk.fi.

this adverse behavior, 8 devices of different plate sizes were selected for optical characterization of the IP and out-of-plane (OP) vibration fields (preliminary findings reported in Ref. 10). The results of the optical measurements indicate a coupled resonance between the resonator plate and the anchors. This finding is further supported by a good fit of an analytic model of two coupled resonators with the experimental data.

The resonator structure is illustrated in Fig. 1(a). The fabricated set consists of resonators of 64 different sizes; the side length of the plate is varied from $L = 131\ \mu$m to $L = 320\ \mu$m in steps of $3\ \mu$m. This plate size range corresponds to a designed SE frequency range from 13 to 32 MHz. The design and the dimensions of the anchors were kept the same in all resonators. Each size variation was replicated 10 times on a single wafer, and the replicas were distributed over the whole wafer. The fabrication process is described in Ref. 3.

The electrical responses of approximately 1200 resonators from two wafers were measured with an impedance analyzer (Agilent Technologies A4294). The resonance frequency f_0, motional resistance R_m, quality factor Q, and the parallel capacitance C_0 were determined by fitting an electrical equivalent circuit model of the resonator [see inset in Fig. 1(b)] to the measured impedance data.

Eight devices with L ranging from 137 μm to 305 μm (in steps of 24 μm) were selected for laser probe measurements. The laser probing was carried out using a scanning Michelson laser interferometer.[11] The instrument enables amplitude and phase measurements of both the OP[12] and IP components[13,14] of the surface vibrations.

The OP and IP scan areas and their relation to the sample geometry are depicted in Fig. 1(b). To get an overview of the acoustic behavior of the sample, the OP data were first measured over the whole resonator [scan area I in Fig. 1(b)] including the resonator plate, anchors, and a part of the substrate. The IP vibration fields were then obtained from the resonator plate (scan area II). In addition, both vibration components were measured over the top-right anchor and a part of the resonator plate (scan area III). All the optical measurements were carried out at low pressure (<0.2 mbar) and at room temperature.

An analytic spring-mass model of the resonator, in which the contribution of the anchors is excluded (see inset A in Fig. 2), predicts that the resonance frequency of the SE mode is inversely proportional to the plate side length L. In the electrical characterization results, however, a deviation from the expected $1/L$ frequency scaling is observed, see Fig. 2. In particular, at the intermediate plate sizes, $160\ \mu\text{m} < L < 260\ \mu$m, instead of a single resonance, two strong resonances are observed above and below the predicted SE resonance frequency such that the SE mode branch appears to split into two distinct frequency branches. In addition, for these plate dimensions, the spread of the resonance frequencies between samples of the same plate size increases when the upper or lower resonance frequency branches diverges away from the expected $1/L$ scaling.

In the eight optically measured samples, despite of the frequency splitting, the IP vibration field of the two branches corresponds to what is characteristic to the SE mode, except for the $L = 185\ \mu$m plate size at the lower frequency branch and for the $L = 233\ \mu$m and $L = 257\ \mu$m plate sizes at the higher frequency branch (see the symbolic representation in Fig. 2). These three non-SE modes are observed to vibrate strongly in the OP direction, indicating that another mode, with a strong OP component, is excited instead of the SE mode at these plate dimensions.

It is also observed that the IP vibration amplitudes and the electrically characterized resonances are stronger for the branch that is closer to the predicted frequency of the SE mode. The electrical Q values of the resonances on the stronger branch are typically between 12 000 and 18 000 and R_m between 80 and 200 Ω at a pressure of <10 mbar, whereas on the weaker branch they are significantly worse, $Q \sim 100$–1000 and $R_m > 1\ \text{k}\Omega$.

The laser probing measurements reveal an increased vibration activity at the anchors within the 20–22 MHz frequency range for all plate sizes. In this frequency range, several resonances are observed that feature stronger IP and OP vibration amplitudes at the anchors than at the resonator plate. An example of the frequency response of such a resonance is illustrated in Fig. 2 (enlarged in the inset E).

The IP phase data give further evidence on the role of the increased anchor activity at the 20–22 MHz frequency range to the splitting of the SE mode. The phase data in insets C and D of Fig. 2 show that the resonator plate and the anchor are moving in opposite phase on the higher-frequency branch, whereas on the lower-frequency branch, they vibrate in phase. This would indicate that the resonances on the upper and lower branches are the two eigenmodes of a coupled oscillation between the SE mode and a parasitic anchor mode. The trends of the behavior of the two frequency branches also suggest that this anchor mode exists between 20 and 22 MHz.

A coupled two-resonator model, depicted in inset B of Fig. 2, was used to give further support to our conclusion. A spring-mass system with an effective mass m_1 and a spring constant k_1 describes the SE mode of the resonator plate. When another spring-mass system (k_2, m_2) is introduced in the model to take into account the anchor, this coupled resonator model results in a good fit to the electrically measured resonance frequency data.

The extensive electrical and laser probe characterizations of this study have provided us with valuable information on the anchor resonance effects to the operation of the MEMS plate resonator. It is evident that even small and flexible anchors may have a significant impact on the resonance behavior of the massive plate (relative to the anchors), at least in the case when the resonator plate is not anchored at a nodal point of the plate's vibrational motion. As seen from the electrical data in Fig. 2, the deviation of the stronger SE resonance branch from the $1/L$ scaling starts already at around $L = 170\ \mu$m (upper branch) and $L = 230\ \mu$m (lower branch), although the resonance frequencies are more than 1 MHz away from the 20 to 22 MHz frequency range where the anchors are active.

The coupling between the SE mode and a parasitic anchor resonance leads to unwanted consequences. First of all, certain operation frequencies cannot be achieved by simply scaling the size of the resonator plate unless the anchor design is changed accordingly. More importantly, the spread of the SE

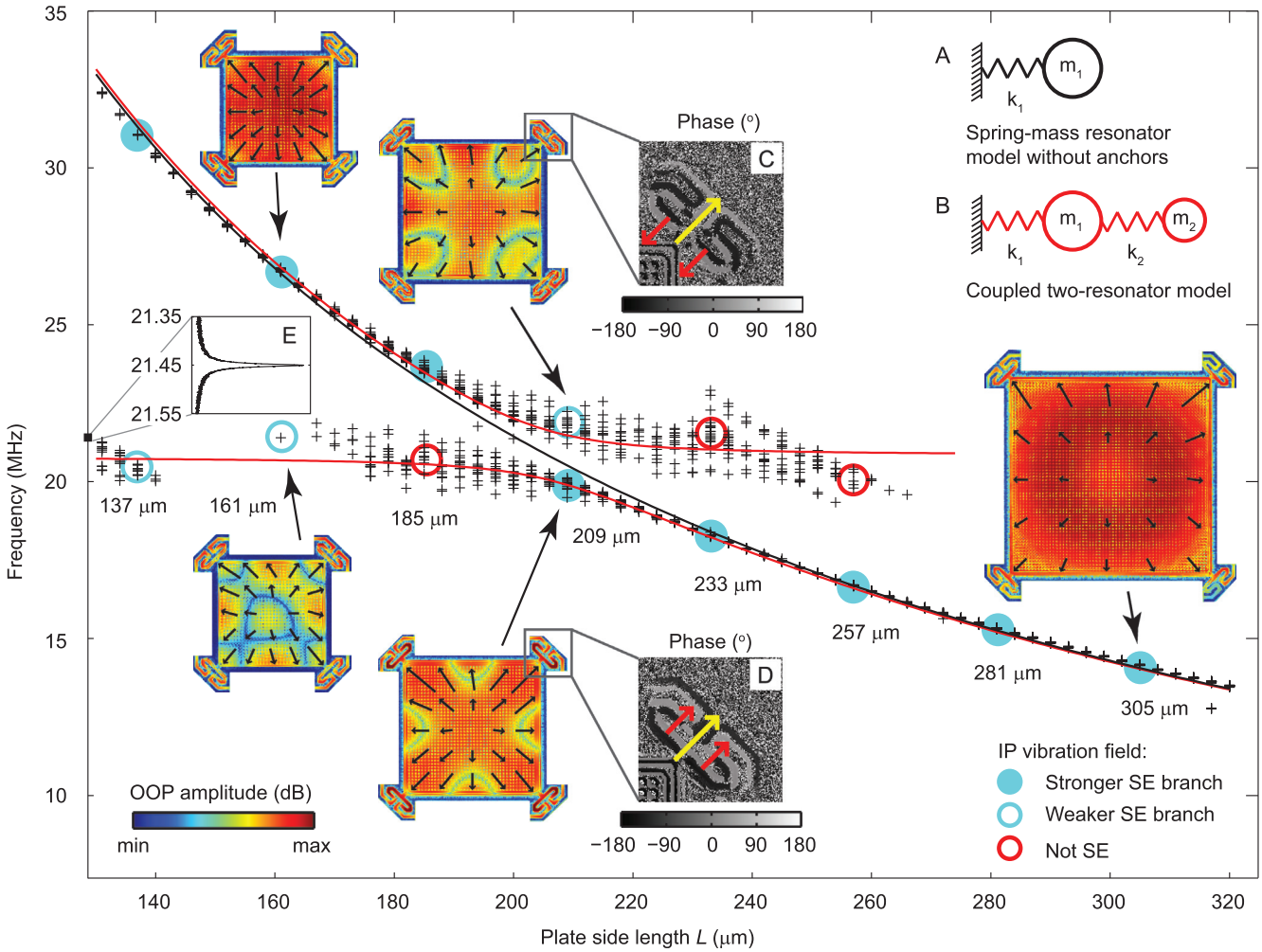

FIG. 2. (Color) The electrical characterization and laser probing results. The electrically characterized resonance frequencies (black "+") are plotted as a function of the plate side length L. Only the resonances corresponding to the two frequency branches closest to the pure SE mode frequency curve (black line) predicted by the single spring-mass model (shown in inset A) are presented. The red curves represent the least squares fit of the coupled resonator model (shown in inset B) to the electrical data. The measured OP (colormap) and IP amplitude data (black arrows on the OP data) of selected plate sizes are shown as insets. To visualize the vibration fields, each OP data figure has a separate logarithmic scaling normalized to its maximum OP amplitude, and also the lengths of the arrows indicating the IP fields have a separate linear scaling for each data figure. Insets C and D: The IP phase data of the top-right anchor of the $L = 209\ \mu$m resonator. The instantaneous movement directions of the anchor and the resonator plate are depicted with red and yellow arrows. Inset E: Frequency sweep of the IP vibration amplitude of a selected resonance within the 20-22 MHz range, in which increased anchor activity is observed (measured from the top-right anchor).

resonance frequencies between resonator samples of the same size is too high for frequency control and timing applications in the region where the SE frequency deviates from the $1/L$ relationship due to the mode coupling. In this study, this frequency spread is unsatisfactorily high over an operational frequency range of 19–25 MHz. To avoid the adverse effects of the anchor-plate coupling, a large frequency margin between the main and anchor resonance is therefore required.

L.L. acknowledges Aalto University School of Science and Technology for scholarships.

[1]V. Kaajakari, T. Mattila, A. Oja, J. Kiihamäki, and H. Seppä, IEEE Electron Device Lett. **25**, 173 (2004).
[2]G. K. Ho, R. Abdolvand, A. Sivapurapu, S. Humad, and F. Ayazi, J. Microelectromech. Syst. **17**, 512 (2008).
[3]A. Jaakkola, P. Rosenberg, S. Asmala, A. Nurmela, T. Pensala, T. Riekkinen, J. Dekker, T. Mattila, A. Alastalo, O. Holmgren, and K. Kokkonen, in *Proceedings of the IEEE Ultrasonics Symposium*, Beijing, China, November 2–5, 2008 (IEEE, New York, 2008), pp. 717–720.
[4]Z. Hao, A. Erbil, and F. Ayazi, Sens. Actuators, A **109**, 156 (2003).
[5]D. S. Bindel, E. Quévy, T. Koyama, S. Govindjee, J. W. Demmel, and R. T. Howe, in *Proceedings of the IEEE MEMS 2005* (IEEE, Inc., Miami, Florida, U.S, 2005), pp. 133–136.
[6]J. E.-Y. Lee, J. Yan, and A. A. Seshia, in *Proceedings of Eurosensors XXII*, Dresden, Germany, September 7–10, 2008, pp. 536–539.
[7]L. Khine, M. Palaniapan, and W -K. Wong, in *Proceedings of the Solid-State Sensors, Actuators and Microsystems Conference*, Lyon, France, June 10–14, 2007, pp. 1753–1756.
[8]L. Khine and M. Palaniapan, J. Micromech. Microeng. **19**, 015017 (2009).
[9]A. Jaakkola, J. Lamy, J. Dekker, T. Pensala, L. Lipiäinen, and K. Kokkonen, in *Proceedings of the IEEE International Frequency Control Symposium*, Newport Beach, California, USA, June 1–4, 2010 (IEEE, New York, 2010), pp. 410–414.
[10]L. Lipiäinen, K. Kokkonen, O. Holmgren, and M. Kaivola, in *Proceedings of the IEEE Ultrasonics Symposium*, San Diego, California, USA, October 11–14, 2010 (IEEE, New York, 2010), pp. 416–419.
[11]J. V. Knuuttila, P. T. Tikka, and M. M. Salomaa, Opt. Lett. **25**, 613 (2000).
[12]L. Lipiäinen, K. Kokkonen, and M. Kaivola, J. Appl. Phys. **108**, 114510 (2010).
[13]O. Holmgren, K. Kokkonen, T. Mattila, V. Kaajakari, A. Oja, J. Kiihamäki, J. V. Knuuttila, and M. M. Salomaa, Electron. Lett. **41**, 16 (2005).
[14]O. Holmgren, K. Kokkonen, T. Veijola, T. Mattila, V. Kaajakari, A. Oja, J. V. Knuuttila, and M. Kaivola, J. Micromech. Microeng. **19**, 015028 (2009).